

# Understanding and quantifying focused, indirect groundwater recharge from ephemeral streams using water table fluctuations

Cuthbert, Mark

DOI:

[10.1002/2015WR017503](https://doi.org/10.1002/2015WR017503)

License:

Creative Commons: Attribution (CC BY)

*Document Version*

Peer reviewed version

*Citation for published version (Harvard):*

Cuthbert, M 2016, 'Understanding and quantifying focused, indirect groundwater recharge from ephemeral streams using water table fluctuations', *Water Resources Research*. <https://doi.org/10.1002/2015WR017503>

[Link to publication on Research at Birmingham portal](#)

**Publisher Rights Statement:**

Eligibility for repository: Checked on 11/3/2016

**General rights**

Unless a licence is specified above, all rights (including copyright and moral rights) in this document are retained by the authors and/or the copyright holders. The express permission of the copyright holder must be obtained for any use of this material other than for purposes permitted by law.

- Users may freely distribute the URL that is used to identify this publication.
- Users may download and/or print one copy of the publication from the University of Birmingham research portal for the purpose of private study or non-commercial research.
- User may use extracts from the document in line with the concept of 'fair dealing' under the Copyright, Designs and Patents Act 1988 (?)
- Users may not further distribute the material nor use it for the purposes of commercial gain.

Where a licence is displayed above, please note the terms and conditions of the licence govern your use of this document.

When citing, please reference the published version.

**Take down policy**

While the University of Birmingham exercises care and attention in making items available there are rare occasions when an item has been uploaded in error or has been deemed to be commercially or otherwise sensitive.

If you believe that this is the case for this document, please contact [UBIRA@lists.bham.ac.uk](mailto:UBIRA@lists.bham.ac.uk) providing details and we will remove access to the work immediately and investigate.

1 **Understanding and quantifying focused, indirect groundwater recharge from**  
2 **ephemeral streams using water table fluctuations**

3 M. O. Cuthbert\*<sup>1,2</sup>, R. I. Acworth<sup>2</sup>, M. S. Andersen<sup>2</sup>, J. Larsen<sup>2,3</sup>, A. McCallum<sup>4</sup>, G. C. Rau<sup>2</sup>,  
4 J. H. Tellam<sup>1</sup>

5 1. School of Geography, Earth and Environmental Sciences, University of Birmingham,  
6 Edgbaston, Birmingham B15 2TT, UK

7 2. Connected Waters Initiative Research Centre, UNSW Australia, 110 King St, Manly Vale,  
8 NSW 2093 Australia

9 3. School of Geography, Planning, and Environmental Management, University of  
10 Queensland, Brisbane, Australia

11 4. Affiliated with Connected Waters Initiative Research Centre, UNSW Australia, 110 King  
12 St, Manly Vale, NSW 2093 Australia.

13 \*Corresponding author: m.cuthbert@bham.ac.uk

14

15 **Key Points**

- 16 • A water table fluctuation method to quantify indirect recharge is presented  
17 • Indirect recharge decreases almost linearly away from a semi-arid mountain front  
18 • This spatial pattern is persistent both in the long term and on an event basis

19

20 **Keywords**

21 Groundwater recharge, ephemeral stream, water table fluctuation, semi-arid hydrology,  
22 indirect recharge, focused recharge, dryland hydrology, mountain front

23 **Abstract**

24 Understanding and managing groundwater resources in drylands is a challenging task, but  
25 one that is globally important. The dominant process for dryland groundwater recharge is  
26 thought to be as focused, indirect recharge from ephemeral stream losses. However, there is a  
27 global paucity of data for understanding and quantifying this process and transferable  
28 techniques for quantifying groundwater recharge in such contexts are lacking. Here we  
29 develop a generalised conceptual model for understanding water table and groundwater head  
30 fluctuations due to recharge from episodic events within ephemeral streams. By accounting  
31 for the recession characteristics of a groundwater hydrograph, we present a simple but  
32 powerful new water table fluctuation approach to quantifying focused, indirect recharge over  
33 both long term and event timescales. The technique is demonstrated using a new, and  
34 globally unparalleled, set of groundwater observations from an ephemeral stream catchment  
35 located in NSW, Australia. We find that, following episodic streamflow events down a  
36 predominantly dry channel system, groundwater head fluctuations are controlled by pressure  
37 redistribution operating at three timescales from vertical flow (days to weeks), transverse  
38 flow perpendicular to the stream (weeks to months) and longitudinal flow parallel to the  
39 stream (years to decades). In relative terms, indirect recharge decreases almost linearly away  
40 from the mountain front, both in discrete monitored events as well as in the long term  
41 average. In absolute terms, the estimated indirect recharge varies from 80 to 30 mm/a with  
42 the main uncertainty in these values stemming from uncertainty in the catchment scale  
43 hydraulic properties.

44

## 45 **1. Introduction**

46 Dryland regions (semi-arid and arid regions but excluding hyper-arid deserts) are expanding  
47 and now represent ~35% of the global landmass, support a population of around 2 billion  
48 people (90% of which live in developing countries), 50% of the world's livestock, 44% of all  
49 cultivated land and contain some of the most important wetlands in the world [*Hassan et al.*,  
50 2005]. Water scarcity is becoming more critical in dryland areas due to population growth  
51 and urbanisation, increasing irrigation demands and climate change [*Scanlon et al.*, 2006;  
52 *Taylor et al.*, 2013]. In the wider Earth Science context, understanding groundwater recharge  
53 processes in drylands is also important for the interpretation of paleoclimatic proxy archives  
54 [*Cuthbert et al.*, 2014], and their longer term sensitivity to change. Furthermore,  
55 understanding the relationships between climate and groundwater availability in drylands  
56 may enable us to understand better our own origins as human beings [*Cuthbert and Ashley*,  
57 2014]. However, the understanding and quantification of groundwater recharge processes in  
58 dryland areas remains a major challenge worldwide [*Wheater et al.*, 2010].

59 In drylands the climate has large atmospheric water demands and temperature contrasts,  
60 surface water flows are infrequent but potentially damaging and populations are sparse and  
61 often have limited economic resources [*Wheater et al.*, 2010]. Groundwater recharge in  
62 drylands predominantly occurs via leakage from ephemeral streams [*Simmers*, 1997; 2003].  
63 Recharge can also occur more diffusely under the right conditions. For example where  
64 sufficient preferential flow pathways exist to enable flow to by-pass otherwise dry soil  
65 profiles, or where soil moisture deficits are limited due to thin soils or lack of vegetation  
66 [*Cuthbert and Tindimugaya*, 2010; *Cuthbert et al.*, 2013], or in Mediterranean climates with a  
67 winter rainy season when evapotranspirative losses are lower [*van Loon and van Lanen*,  
68 2013]. However, these diffuse processes are, arguably, more widely understood and already  
69 successfully included in large scale hydrological models, while the major areas of uncertainty

70 exist in areas where recharge from surface-water bodies such as ephemeral streams  
71 dominates [*Döll and Fiedler, 2007; Epstein et al., 2010; Wheatler et al., 2010*]. Following  
72 Healy [2010] here we use the term 'focused recharge' to refer to any recharge from a surface  
73 water body, and 'indirect recharge' as a sub-type of focused recharge whereby recharge  
74 occurs due to infiltration from streambeds such as the ephemeral streams that drain semi-arid  
75 mountain front systems.

76 Systematic, multi-year observations of groundwater dynamics in ephemeral stream  
77 catchments are very rare and only reported for a few sites worldwide [*Besbes et al., 1978;*  
78 *Carling et al., 2012; Goodrich et al., 2004; Pool, 2005; Shentsis and Rosenthal, 2003*]. Most  
79 dryland hydrological studies have been 'top down', attempting to characterise groundwater  
80 recharge using a water balance approach based on surface measurements. Such methods are  
81 complicated by the inherent non-linearities in predicting rainfall-runoff relationships, the  
82 difficulties of measuring flows and therefore transmission losses accurately in such  
83 environments, and transience in the nature of streambed losses [*Shanafiield and Cook, 2014*].  
84 Where transmission losses can be measured well or predicted, estimations of recharge are  
85 then hampered by the difficulty of estimating transpiration losses and/or lateral subsurface  
86 flow behaviour due to alluvial structures [*Telvari et al., 1998*]. Furthermore, upscaling from  
87 point scale measurements to larger scales can be highly problematic [*McCallum et al., 2014*].

88 In contrast, observations of the water table fluctuations of a catchment can provide the most  
89 direct measure possible of the recharge behaviour, as they integrate the recharge response  
90 over a spatial footprint much larger than that of the measurement (borehole) scale. Estimating  
91 indirect recharge from time series of groundwater level measurements has been the subject of  
92 much research, but almost exclusively focused on inverse solutions of the transient mounding  
93 equations in various forms [*Abdulrazzak and Morel-Seytoux, 1983; Dillon and Liggett, 1983;*  
94 *Hantush, 1967; Moench and Kisiel, 1970*] However, this previous work has not generally

95 accounted for the background groundwater recession behaviour or lateral boundary  
96 conditions. Furthermore, published studies are mostly based on data from a single piezometer  
97 or single event, therefore restricting its applicability. Finally, the available analytical  
98 approaches struggle with the complexity of the form of the input function for time varying  
99 recharge.

100 In this paper we first develop a generalised conceptual model for understanding water table  
101 fluctuations in ephemeral stream catchments using insights gained from analytical and  
102 numerical models of idealised aquifers. By accounting for the recession characteristics of a  
103 groundwater hydrograph we then present a simple but powerful new approach to quantifying  
104 indirect recharge separately over both the long term and on an event basis. This model is then  
105 tested using a unique monitoring database of groundwater dynamics from an ephemeral  
106 stream catchment in NSW, Australia.

## 107 **2. Theoretical Background**

### 108 **2.1 The water table fluctuation method for quantifying recharge**

109 The basis of the water table fluctuation (WTF) technique for quantifying recharge is the  
110 following equation:

$$111 \quad R = S_y \frac{\partial h}{\partial t} + D \quad (1)$$

112 where  $R$  is the rate of recharge [ $\text{LT}^{-1}$ ],  $S_y$  is specific yield [-],  $t$  is time [T],  $h$  is hydraulic head  
113 [L] and  $D$  is the rate of net groundwater drainage (or ‘rate of groundwater flux recession’)  
114 [ $\text{LT}^{-1}$ ] [Cuthbert, 2010]. This assumes that changes in groundwater level in an aquifer are  
115 controlled solely by the balance of recharge and net groundwater drainage away from a given  
116 observation point and ignores other factors such as entrapped air, barometric fluctuations or  
117 local groundwater abstraction. The main limitations of the WTF method stem from

118 difficulties of defining and estimating specific yield, and accounting for the drainage term ( $D$ )  
119 robustly [Healy and Cook, 2002].

## 120 **2.2 The general form of water table fluctuations in catchments dominated by indirect** 121 **episodic recharge**

122 An improved understanding and estimation of  $D$  has recently been proposed for the 1-D  
123 groundwater flow equations under uniform recharge [Cuthbert, 2010; 2014]. However, an  
124 adequate method for dealing with the recessional characteristics of a catchment in which  
125 recharge is dominated by losses from an ephemeral stream has not so far been proposed. It is  
126 therefore addressed here with regard to the idealised 2-dimensional aquifer shown in  
127 Figure 1. It is bounded at one end (at  $x = L$ ) by a no flow boundary – this may represent the  
128 edge of an alluvial aquifer abutting a mountain front for example, typical in headwater  
129 ephemeral stream settings [Pool, 2005; Simmers, 1997]. The aquifer episodically receives  
130 surface runoff via a stream channel flowing in the  $x$ -direction from higher elevations across  
131 this boundary which is then received by the aquifer beneath via streambed infiltration during  
132 episodic flow events. The downstream boundary condition at ( $x = 0$ ) is a constant head  
133 boundary representing a typical discharge zone such as the transition to a perennial stream,  
134 wetland or terminal lake. The lateral boundaries are no flow, thus the system is representative  
135 of a series of parallel ephemeral streams, again a reasonable simplification in a dryland  
136 setting. The linearised groundwater flow equation in 2-dimensions for such an aquifer, here  
137 assumed to be homogeneous and isotropic, may be written as follows:

$$138 \quad R = S_y \frac{\partial h}{\partial t} - T \left( \frac{\partial^2 h}{\partial x^2} + \frac{\partial^2 h}{\partial y^2} \right) \quad (2)$$

139 where  $T$  is transmissivity [ $L^2T^{-1}$ ], and  $x$  and  $y$  are orthogonal length variables [ $L$ ] as shown in  
140 Figure 1. This linearisation assumes that the fluctuations in water table elevations are small  
141 compared with the saturated thickness of the aquifer.

142 For some time during and after an episodic streamflow event we would expect a groundwater  
143 mound to rise and decay in the vicinity of the stream. Assuming that the recharge occurs  
144 along the length of the stream, it is effectively acting as a line source during the recharge  
145 period. We would thus expect the pressure wave generated to propagate transversely towards  
146 the lateral boundaries, at a distance  $W$  in the direction perpendicular to the stream, with an  
147 aquifer response time (ART), or time constant, of  $t_{lat} = W^2 S_y / T$  [Currell *et al.*, 2014;  
148 *Domenico and Schwartz*, 1998; *Rousseau-Gueutin et al.*, 2013]. This aquifer event response  
149 will be superimposed on a longer term background recession acting longitudinally in the  
150 direction parallel to the stream due to drainage to the perennial stream reach downstream,  
151 with a characteristic ART of  $t_{long} = L^2 S_y / T$ .

152 It is clear from a comparison of Equations 1 and 2 that the groundwater flux recession rate,  
153  $D$ , is given by:

$$154 \quad D = -T \left( \frac{\partial^2 h}{\partial x^2} + \frac{\partial^2 h}{\partial y^2} \right) \quad (3)$$

155 The first and second terms on the RHS of Equation 3 express the superposition of the  
156 longitudinal recession and the transverse recession respectively.

157 To illustrate these concepts the scenario described above and illustrated in Figure 1 has been  
158 modelled numerically using COMSOL Multiphysics (v5.1). The indirect recharge was  
159 simulated as an imposed flux boundary condition across a constant width of 20 m. This  
160 implicitly assumes that there is insignificant lateral spreading of the wetting front beneath the  
161 stream which is reasonable for cases where the depth to water table is less than the width of  
162 the channel [Nimmo *et al.*, 2002]. However the applied recharge from the channel varied in  
163 space along the reach, with recharge decreasing linearly to zero between the upstream and  
164 downstream boundaries - an arbitrary distribution but one which mirrors the finding of  
165 previous research, that indirect recharge decreases away from runoff source areas such as



166 mountain blocks [Simmers, 1997]. A long time series of identical episodic recharge events,  
167 each with a constant flux and duration, was modelled to bring the system to a quasi-steady  
168 state. The heads at points 1-4 were then output from the model for the last event and are  
169 shown as hydrographs in Figure 2. The parameters used are given in the legend for Figure 1.

170 Figure 2 shows how the background (longitudinal) recession is expressed as a straight line  
171 with a transverse mounding event superimposed upon it. The timescale for the decay of the  
172 mound can be estimated using an analytical solution. The analogous idealised problem of the  
173 1-D redistribution of heads following a change in flux at one boundary (i.e.  $y=0$  at the  
174 stream), and a no flow boundary at  $y=W$  (i.e. an aquifer half space assuming parallel  
175 streams) is given by Bruggeman's Equation 135.02 [Bruggeman, 1999]. Using this solution, it  
176 is possible to show that 99% of the transience created by a change in flux at the stream  
177 boundary will have decayed away within  $t = t_{mound} \sim W^2 S_y / (2T)$  (i.e. half of  $t_{lat.}$ ) since the  
178 change in flux. For the present case of the ideal aquifer example plotted in Figure 2,  
179  $t_{mound} \sim 100$  days.

180 Furthermore, where recharge is distributed evenly across a catchment, recent theoretical work  
181 [Cuthbert, 2014] shows that straight line recession behaviour is expected prior to  
182  $t_{lin} = x^2 S_y / (16T)$  since a recharge event occurred, where  $x$  is the distance from the monitoring  
183 point to the downstream fixed head boundary. In our modelled example,  $L$  is significantly  
184 greater than  $W$ , as you would expect in most natural settings, and thus  $t_{mound}$  is smaller than  $t_{lin}$   
185 over much of the catchment. Hence, the straight line recession is observable under such  
186 conditions, as long as the time between recharge events is greater than  $t_{mound}$ . A further point  
187 worth noting here is that straight line recessions are also expected in contexts where flow  
188 lines are divergent [Cuthbert, 2014]. Thus where an aquifer is bounded by streams that are  
189 not parallel, the mounding timescales may vary along the length of the streams, but the long

190 term recession would still be expected to be linear at early times following the cessation of  
 191 recharge.

192 Straight line background recessions are observed in our synthetic example in line with the  
 193 theory developed for evenly distributed recharge, despite the modelled recharge actually  
 194 varying spatially. It is important to demonstrate that this feature of longitudinal recessions is  
 195 a generally applicable one for the case of spatially variable recharge. Thus, additional  
 196 analysis is needed as outlined in the next section.

### 197 **2.3 Groundwater flux recession in catchments with spatially variable recharge**

198 An expression for the recession of an ideal 1-D aquifer from an arbitrary initial condition is  
 199 given by equation (10) of Venetis [Venetis, 1971]. In order to test the possible form of the  
 200 longitudinal recession for the case considered above (i.e. recharge increasing linearly from  
 201 zero at a downstream constant head boundary condition ( $h = 0$ ) at  $x = 0$  to  $R_{max}$  at  $x = L$ ) it is  
 202 useful to set the initial condition ( $h_0(x)$ ) to the head distribution under steady state conditions.  
 203 For  $R = R_{max}x/L$ , then it is straightforward to show that:

$$204 \quad h_0(x) = -\frac{R_{max}x^3}{6LT} + \frac{R_{max}Lx}{2T} \quad (4)$$

205 Venetis (1971, equation 10) gives the following expression for the variation in head as:

$$206 \quad h(x, t) = \frac{1}{L} \sum_{n=1,3,5,\dots} e^{\frac{-n^2\pi^2Tt}{4SL^2}} \sin\left(\frac{n\pi x}{2L}\right) \int_0^{2L} h_0 \sin\left(\frac{n\pi x}{2L}\right) dx \quad (5)$$

207 From this equation, the conditions under which spatially variable recharge should produce  
 208 straight line recessions can be analysed. Since we are only considering 1-D (longitudinal)  
 209 flow in this case, (i.e. just considering the recession which occurs after any mounding due to  
 210 indirect recharge, and variation in head in the y-direction, has dissipated) the net groundwater  
 211 drainage can be simplified to:

212 
$$D = -T \frac{d^2h}{dx^2} \quad (6)$$

213 Equations 4 to 6 have been used to plot Figure 3 with  $D$  normalised to the recharge value at  
214 the mid-point of the model domain ( $x/L=0.5$ ). This shows how the modelled groundwater  
215 flux recession rate varies following a recharge event relative to the initial recharge rate across  
216 a range of ARTs. Values close to 1 on the vertical axis thus indicate that the recession is a  
217 straight line and accurately predicts the spatially varying recharge rate.

218 This shows that for some time following cessation of recharge, the straight line recessions are  
219 a direct indicator of the variation of the spatial variability in long term recharge. Furthermore,  
220 this analysis indicates that even for this case of spatially varying recharge,  $t < t_{lin}$  [Cuthbert,  
221 2014] can provide a reasonable (and conservative) measure of the length of time straight line  
222 recessions can be expected to last.

#### 223 **2.4 A water table fluctuation method for quantifying indirect recharge**

224 Based on the preceding theory, we can now propose a new WTF approach to estimating  
225 episodic indirect recharge. As with any WTF recharge estimation methodology, it should  
226 only be used if a robust conceptual model warrants it. Thus, as per the methodology outlined  
227 by [Cuthbert, 2010] for estimating diffuse recharge using WTFs, the first steps to be taken  
228 should be delineating the main hydrogeological boundaries, considering the likely controls on  
229 recharge due to the presence of superficial deposits and the climatic context, and utilising  
230 estimations of aquifer properties where possible. Furthermore, the time series of groundwater  
231 level data to be used must be of sufficient temporal resolution, representative of the local  
232 water table position, and sufficiently distant from the influence of pumping wells.

233 The analytical and numerical models of an idealised catchment described above, suggest that  
234 where a straight line groundwater level recession is observable, it can be used in two ways to  
235 estimate indirect groundwater recharge:

236 1. The slope of the straight line recession can be used to estimate the ‘long term’ ratio of  $R/S_y$ ,  
237 (or the actual recharge if  $S_y$  is known) by the following equation:

$$238 \quad R_{av} = S_y \frac{\partial h}{\partial t} \quad (7)$$

239 Since the antecedent history of the system is not necessarily known, the meaning of ‘long  
240 term’ cannot always be precisely determined. However, as Figure 4 indicates, away from the  
241 fixed head boundary, the aquifer damps out variations in recharge so that significant  
242 variations in flux recession rate only occur due to recharge variations with periods less than  
243 the ART. Hence, away from a fixed head boundary, observation of a straight line recession  
244 and use of Equation 7 will provide an estimate of the recharge occurring over the previous  
245 time period defined by the ART (Figure 4).

246 2. On an event basis, the background recession can be added to a groundwater hydrograph  
247 time series to reveal the change in head due exclusively to event recharge from the stream.  
248 This is illustrated in Figure 5, where the effect of the long term recession rates have been  
249 removed in this way from the groundwater hydrographs already shown in Figure 2. If the  
250 system is behaving in the manner expected by the conceptual model outlined, for  $t > t_{mound}$ ,  
251 the result should be a step change in head ( $\Delta h$ ) where:

$$252 \quad R_{event} = S_y \Delta h \quad (8)$$

253 Figure 5 indicates that, with the longitudinal recession removed, significant head increases  
254 still occur nearer to the stream due to the transverse spreading of the pressure wave generated  
255 by the flow event (hydrographs 1 and 3). However, further away from the stream

256 (hydrographs 2 and 4) this effect becomes almost unnoticeable, with the response now  
257 resembling a gradual step change in head.

258 Both techniques ultimately rely on knowing the value of  $S_y$  for estimating actual recharge and  
259 this can be challenging to obtain at the right spatial scale. However,  $S_y$  can be estimated from  
260 the definition of  $t_{mound}$  ( $W^2 S_y / (2T)$ ) if  $t_{mound}$  is determined by observation,  $T$  is estimated for  
261 example from a pumping test, and  $W$  from the geometry of the system.

### 262 **3. A case study from Middle Creek, NSW, Australia**

#### 263 **3.1 Catchment context**

264 The catchment has been described in detail previously [*Andersen and Acworth, 2009; Rau et*  
265 *al., 2010*] and is only briefly summarised here. Middle Creek (via Horsearm Creek) is an  
266 ephemeral tributary to Maules Creek, itself a tributary to the Namoi river in the headwaters of  
267 the Murray Darling Basin, NSW, Australia (Fig. 6). The Nandewar Range (part of the Great  
268 Dividing Range) to the north-east receives approximately 1100 mm per year of precipitation  
269 in the long term. Rainfall is generally well distributed throughout the year, however the  
270 rainfall intensity varies substantially with heavy rains generally occurring in the summer  
271 months (Dec – Feb). The rainfall is also influenced by longer term fluctuations in the El Nino  
272 Southern Oscillation Index (ENSO), with higher than average rainfalls in the positive phase  
273 (La Nina) and lower than average rainfalls in the negative phase (El Nino).

274 Large storm events generate runoff from the steep headwaters of Middle Creek catchment  
275 which is comprised of Miocene volcanic rocks overlain by thin soils with forested land use.  
276 Flow is delivered across the mountain front (defined by a thrust fault) and onto a moderate  
277 gradient (1 to 2%), Quaternary age, alluvial fan up to 40 m thick. This overlies Permian  
278 sedimentary deposits (claystones, siltstones, sandstones, conglomerates and coal measures)

279 and Carboniferous crystalline rocks, meta-sediments and volcanic deposits. The degree of  
280 hydraulic connectivity between the Quaternary alluvium and these underlying formations is  
281 presently unknown. As can be seen in Figure 6, the land downstream of the mountain front is  
282 largely cleared for grazing, except for a narrow vegetated zone adjacent to the creek. A well  
283 delineated ephemeral channel has cut through clay rich soils which otherwise blanket the  
284 alluvium. The main channel is typical of an episodic high energy stream comprising sand and  
285 gravel deposits often forming pool-riffle sequences and cobble to boulder size lag. Ephemeral  
286 flows have been observed to extend all the way to the confluence with Horsearm Creek and  
287 Maules Creek. Rainfall on the alluvial fan itself decreases to the southwest away from the  
288 Nandewar range. At Middle Creek Farm, the recent record indicated 522 mm/a for 2014,  
289 Bellevue farm situated further downstream averages 534 mm/a, and both are in contrast to the  
290 912 mm/a for Mt Kaputar in the catchment headwaters (see Figure 6 for locations).

291 For the time series available, Middle Creek flows when the cumulative rainfall in the month  
292 prior exceeds around 140 mm and the majority of runoff is assumed to be generated in the  
293 steep and low permeability mountain headwaters. The regional hydraulic gradient indicated  
294 by available groundwater level data is approximately northeast to southwest. There is little  
295 groundwater pumping in the Middle Creek area itself. However Middle Creek is just one of a  
296 series of ephemeral streams draining into Maules Creek and providing recharge to aquifers  
297 which are extensively pumped for cotton irrigation in the Namoi valley downstream.

### 298 **3.2 Monitoring installations & testing methods**

299 Six 0.168 m diameter boreholes (Fig. 6) were drilled in 2012 using an air flush  
300 rotary/hammer method with advancing steel casing and installed with either two or four  
301 multilevel piezometers, each screen being hydraulically isolated using bentonite seals. After  
302 completion, the piezometers were developed by air-lifting using a compressor. Care was

303 taken not to blow air into the screened section of the piezometers. Air-lifting was continued  
304 until the discharged water was clear. Details of the resulting 20 piezometers are given in the  
305 Supporting Information. The drill cuttings revealed that the alluvium comprises a highly  
306 heterogeneous layered system of mixed gravel, sand, clay and silt. The large variation in  
307 grainsize is as expected given the alluvial fan depositional setting.

308 Every piezometer was monitored at 15 minute frequency using Solinst Leveloggers,  
309 compensated using a barometric logger situated in a borehole at East Lynne (BH20) which  
310 recorded air pressure at exactly the same times. This was hung in the piezometer at  
311 approximately 2 mbgl to avoid large temperature variations and thereby minimise any diel  
312 artefacts in the pressure data [Acworth *et al.*, 2014], whilst remaining above the water  
313 column. Manual dip-tape measurements were made each time the data were downloaded and  
314 used to check no significant drift in the loggers was occurring. These measurements were  
315 also used, in combination with elevation data of each borehole datum measured using a  
316 Differential GPS, to convert the data to hydraulic head with respect to Australian Height  
317 Datum (AHD).

318 A constant rate pumping test was carried out at Elfin Crossing (BH14, Fig. 6) and analysed  
319 using a transient model. For this analysis the Theis [Theis, 1935] equation was used  
320 incorporating the superposition of an injection image well to implement a recharge boundary  
321 due to the close proximity of the perennial section of Maules Creek (~35 m). The drawdown  
322 data were fitted to the model by varying the hydraulic parameters ( $T$ ,  $S$ ) in order to minimise  
323 the RMSE. Details of the pumping test and analysis can be found in the Supporting  
324 Information.

325 Stream stage was measured adjacent to Boreholes BH20-BH21 at East Lynne using a  
326 Campbell CS450 pressure transducer logged by a Campbell CR1000 since June 2013. Since

327 June 2012, a digital camera placed at East Lynne has been capturing a record of flows in the  
328 creek which can also be used to determine the timing and approximate magnitude of the flow  
329 events. It is noted that some small but greater than zero stage measurements are apparent  
330 between Sep 2013 and March 2014 in the East Lynne stage hydrograph (Fig 7) caused by  
331 temperature driven air pressure differences between the transducer in the creek and the hut on  
332 the creek-bank in which the data logger was housed. However, based on site visits and  
333 photographic evidence from the automated on-site camera, there was no flow in the creek  
334 during this period.

335 A full Campbell weather station was installed next to BH19 at Middle Creek Farm and has  
336 been recording since August 2013.

### 337 **3.3 Groundwater hydrograph dynamics**

338 Time series of heads recorded in every piezometer is shown in Figure 7 alongside the stream  
339 hydrograph at BH20 (East Lynne) and the cumulative rainfall record from Mt Kaputar. We  
340 consider this to be a globally unparalleled dataset with respect to the intensity of groundwater  
341 level data being collected in an ephemeral stream catchment, allowing an unprecedented  
342 insight into its hydrodynamics. More detailed additional plots for nearby groups of  
343 piezometers are given in the Supporting Information Figure S1. Heads varied between  
344 3 and 8 m below ground level with greatest unsaturated zone thickness occurring beneath the  
345 streambed at the most upstream location (BH20 and BH21), and the greatest total unsaturated  
346 zone thickness occurring at the top end of the reach, furthest away from ephemeral streams  
347 (BH22). There is evidence of barometric fluctuations seen in piezometers from BH18-20, but  
348 not in BH17. This suggests the presence of materials with low permeability above the  
349 screened depth in the BH18-20 piezometers [Acworth *et al.*, 2014]. Loading responses also  
350 occur at times of episodic surface flows as indicated by sudden increases in head seen in the



351 groundwater hydrographs, corresponding with sudden stream stage increases in Middle  
352 Creek. This is consistent with the variable lithology encountered during drilling, and the  
353 variability in formation hydraulic conductivity implied by drawdowns observed during  
354 hydrochemical sampling. However, in general the groundwater fluctuations are dominated by  
355 increases coincident with stream flow events in Middle Creek followed by recessions. The  
356 exceptions are BH20\_1 and BH22\_4 which are clearly screened within low permeability  
357 units and therefore show very slow responses in comparison to the other piezometers.  
358 Following an ephemeral flow event, groundwater head changes are characterised by a rapid  
359 increase in gradients between piezometers followed by a more gradual re-equilibration  
360 occurring on three distinct length and time-scales of hydraulic head redistribution. These can  
361 be interpreted as being due to vertical, transverse and longitudinal propagation of the pressure  
362 increase induced by stream flow losses to the underlying alluvium. Vertical downward  
363 hydraulic gradients are initially induced near the creek which then dissipate on the timescale  
364 of days to weeks (for example compare BH17\_1 and BH17\_4 in Figure 7). Transverse  
365 gradients away from the creek dissipate on the timescale of weeks to months, and  
366 longitudinal, down-catchment, gradients are apparent throughout the whole monitoring  
367 period suggesting they persist over longer timescales of years.

368 Consistent with the idealised groundwater hydrograph responses to episodic indirect recharge  
369 described in Section 2 (Figure 1 & 2) there is an observed time lag and amplitude attenuation  
370 with distance away from Middle Creek which is particularly pronounced at the most distant  
371 location from Middle Creek, BH22. Also akin to the idealised hydrographs is the mounding  
372 which occurs after a stream flow event, followed by a gradual transition to a straight line  
373 recession during extended periods of no stream flow. In this case  $t_{mound}$ , estimated as the time  
374 between the cessation of surface flow in the creek and the return to conditions of straight line  
375 groundwater recession, is approximately 135 days. Thus the straight line recession is only

376 seen once in the time series (Feb-Mar 2014) when the time between stream flow events  
377 exceeds this timescale. As shown by the dashed black lines in Figure 7, the steepness of these  
378 long term recessions decreases with distance downstream. For BH20, BH21 & BH22, located  
379 a similar distance from the mountain front, but different distances from Middle Creek (2 m,  
380 37 m and 1111 m, respectively) the mounding behaviour is initially different for each  
381 borehole. However, at later times the recession converges to a remarkably consistent straight  
382 line gradient, as expected from the theoretical considerations discussed above.

383 It is noted that during streamflow events, the head in BH21 rises to a slightly lower absolute  
384 level than the head at BH20, and there is flow away from the creek for the duration of the  
385 flow event, consistent with our conceptual model. However, the recession at BH21 is larger  
386 than that of BH20 which we believe is due to pumping from a nearby stock watering well  
387 located around 60 m west of BH21. It is a very minor abstraction (intermittent, wind-mill  
388 driven pump and the numbers of livestock observed in the vicinity are low) although it  
389 nevertheless appears to produce a local cone of depression which influences the variation in  
390 water level at BH21. This is discussed further in section 3.4 in terms of its implications for  
391 the estimation of recharge. We also note that groundwater use by riparian vegetation remains  
392 unknown at this site. However such water use is certain to contain a significant soil moisture  
393 component, especially during and following recharge events. Any impacts on the water table  
394 by direct groundwater use are therefore likely to be very small relative to the broader trends  
395 observed.

396 Small vertical head gradients, developed in response to streamflow events, are observed in  
397 the logger data at some locations and these differences are consistent with manual dip-tape  
398 measurements, thus not being artefacts of the logged time series. For BH17 and BH20  
399 immediately adjacent to the stream, downward gradients occur after surface water flow  
400 events, consistent with the indirect recharge mechanism proposed, which then dissipate

401 quickly over time since the event. In contrast at BH19, situated 50 m away from the stream,  
402 the gradient is upwards following streamflow events. This is suggestive of water propagating  
403 through a more permeable layer at depth whilst equilibrating vertically as the recharge pulse  
404 dissipates transversely. Since the small vertical gradients equilibrate on a timescale much  
405 shorter than the transverse head gradients, it is a reasonable assumption that the groundwater  
406 level observations are mostly representative of the water table dynamics during the transverse  
407 and longitudinal recession periods. Thus it is reasonable to apply the methodology proposed  
408 in Section 2 which was based on a 2-D representation of an idealised aquifer which assumes  
409 no vertical flow is occurring.

### 410 **3.4 Quantifying recharge using the new methodology**

411 The long term straight line recessions were calculated using the data shown in Figure 7. A  
412 complication in this task was that each borehole hydrograph has a varying degree of  
413 barometric 'noise' in the water level signal. Thus, a purely statistical approach, for example  
414 using a cut-off for a particular coefficient of determination on a linear regression, was not  
415 deemed appropriate. Our approach was, therefore, to identify the time period from which the  
416 hydrographs at different distances from the creek converged onto a consistent linear recession  
417 after a stream flow event and until the groundwater levels began to respond to the next stream  
418 flow event. Since this is somewhat subjective, two reasonable end member times were  
419 selected for start of the linear recession period, in this instance 2 weeks apart from each other,  
420 in order to account for the subjective uncertainty (further apart than this and the mismatch  
421 becomes obvious). The recession rates were then calculated by averaging the incremental  
422 changes in head during the assigned periods. These two recession rates were then 'removed'  
423 from the head time series by adding the calculated values, and the average residual heads  
424 have been plotted in Figure 8. The event based estimates of  $R/S_y$  summed over 2013 were  
425 then calculated from Figure 8 and plotted against the long term estimates in Figure 9, with

426 error bars added to indicate the uncertainty in the analysis due to the variation in the chosen  
427 recession rate. A summary of these values and their uncertainties is given in Table 1.

428 It is noted that the residual head increase at BH21 is larger than that at nearby BH20,  
429 probably due to the minor nearby abstraction as discussed in section 3.3. However, the long  
430 term recession from BH21 eventually begins to converge with those of BH20 and BH22  
431 suggesting that the effect is a transient one which diminishes during dry periods. Hence,  
432 although the derived  $R/S_y$  values for BH21 are likely to be overestimates they are still within  
433 the error bounds for BH20 and BH22.

434 In order to convert the estimates of  $R/S_y$  presented above into actual recharge,  $S_y$  must first be  
435 estimated. A best fit ( $R^2=0.99$ ) value for  $T$  from the pumping test on BH14 was  $115 \text{ m}^2/\text{d}$  (see  
436 Supporting Information). From Figure 7, the mounding timescale at East Lynne can be  
437 estimated as the time from the cessation of flow in the stream until the convergence of the  
438 recessions onto a straight line, which is 135 d with an uncertainty of  $\pm 7$  days as previously  
439 assigned to account for the uncertainty in the choice of the start of the straight line recession  
440 period. The half-space,  $W$ , can be estimated by halving the average distance from Middle  
441 Creek to the adjacent ephemeral creeks. Since there is some convergence of the adjacent  
442 creeks, and therefore variation in  $W$ , with longitudinal distance downstream from the  
443 mountain front (Figure 6), this calculation was only done for the East Lynne location where  
444 the adjacent streams are close to being parallel. Allowing for some uncertainty due to the  
445 slight convergence in the streams we estimate  $W$  to be  $1.6 \text{ km} \pm 0.1 \text{ km}$ . Using the  
446 expression for  $t_{mound}$  given in Figure 2 this implies that the diffusivity ( $T/S_y$ ) is  $\sim 9500 \pm 700$   
447  $\text{m}^2/\text{d}$ . Taking the pumping test value for  $T$  ( $115 \pm 12 \text{ m}^2/\text{d}$ ), yields a value of  $S_y$  of  $0.012 \pm$   
448  $0.003$ . This is reasonable given the prevalence of interbedded clay layers and also a  
449 significant proportion of fines within many layers of the alluvial material encountered in the  
450 catchment. Since a stage hydrograph was only available at East Lynne,  $t_{mound}$  could only be

451 estimated for this location, but the resulting  $S_y$  value was applied to all piezometers. A  
452 summary of the recharge estimates and their uncertainties is given in Table 1.

453 What is immediately apparent is that, assuming  $S_y$  is not varying significantly within the  
454 catchment, the amount of groundwater recharge is generally decreasing with increasing  
455 distance from the mountain front. Furthermore, this trend is consistent between the long term  
456 and event based estimates suggesting that this is a persistent feature of the recharge behaviour  
457 in the catchment. Groundwater recharge for 2013 was lower than the estimated long term  
458 average by around 23% (Figure 9). The long term average value is representative of recharge  
459 occurring over the preceding period given by the ART which, using the above values for the  
460 catchment hydraulic diffusivity and a length of 10 km, is approximately 30 years. Using the  
461 estimate for  $S_y$  of 1.2% enables us to estimate the long term (30 year) recharge in the  
462 catchment using this technique as over 70 mm/a close to the mountain front (BH20-22) and  
463 around 30 mm/a by 6 km further downstream. Similarly, indirect recharge for 2013 has been  
464 calculated and plotted against distance from the perennial downstream boundary indicating  
465 an almost linear relationship (Figure 10). The zero recharge point is defined as the most  
466 upstream perennial section of Horsearm Creek, 2 km upstream of Elfin Crossing. As a reality  
467 check for this system, since the change of recharge with longitudinal distance along the  
468 stream appears to be approximately linear, we have applied equation 4 with  $R_{max} = 68$  mm/a,  
469 the maximum estimated for 2013,  $T = 115$  m<sup>2</sup>/d and  $L = 10\ 000$  m. The computed and  
470 observed heads during a recession period in 2013 are plotted in Figure 10. The comparison is  
471 good given the simplicity of the model, and demonstrates further consistency between the  
472 derived recharge values, estimated aquifer parameters and the groundwater observations.  
473 While we acknowledge the uncertainty in the absolute magnitude in the recharge estimations,  
474 this highly heterogeneous alluvial system is a very challenging one in which to estimate

475 hydraulic properties at the appropriate scale and in more homogeneous aquifers, the  
476 estimation of  $T$  or  $S_y$  should be even more straightforward.

### 477 **3.5. Deviations between real and ideal catchment behaviour**

478 Although the methodology we have presented is potentially very powerful, as with most  
479 analytical methods, several issues arise when applying them to field conditions. For instance,  
480 the model assumes parallel adjacent ephemeral channels but the field example includes  
481 adjacent channels that converge within the study reach. As noted, such deviation in the  
482 geometry will affect the accuracy of the  $t_{mound}$  estimations for calculating hydraulic  
483 parameters. However, straight line recessions are theoretically predicted [Cuthbert, 2014],  
484 and actually observable in catchments with non-uniform flow fields during long term  
485 recession periods as in this field example. Hence such geometries do not affect the  
486 fundamental principle of deriving estimates of the  $R/S_y$  ratio by the method we have  
487 proposed. Other deviations of field situations from the analytical model are also possible such  
488 as differing drainage areas and streamflow timings for adjacent channels, lack of adjacent  
489 channels, and non-parallel impermeable boundaries at differing distances. These should be  
490 considered on a case by case basis, and where significant deviations are found, modifications  
491 to the methodology may be necessary to ensure accurate results.

## 492 **4. Conclusions**

493 We have developed a generalised conceptual model for understanding water table and  
494 groundwater head fluctuations in ephemeral stream catchments and, by accounting for the  
495 recession characteristics of a groundwater hydrograph, presented a simple but powerful new  
496 approach to quantifying indirect recharge both in the long term and on an event basis.  
497 Furthermore, a new, and globally unparalleled, data set of groundwater dynamics in a dryland

498 ephemeral stream catchment from Middle Creek, NSW, Australia has been used to test the  
499 theoretical ideas developed using idealised models.

500 From examination of the extensive field dataset we find that head responses to ephemeral  
501 streamflow events are controlled by pressure redistribution operating at three timescales from  
502 vertical flow (days to weeks), transverse flow perpendicular to the stream (weeks to months)  
503 and longitudinal flow parallel to the stream (years to decades). From application of the new  
504 methods to the field dataset we find that, in relative terms, groundwater recharge increases  
505 linearly away from the mountain front to the perennial stream section, and has a similar  
506 spatial pattern both in the recent events analysed as well as over the longer term. In absolute  
507 terms the long term indirect recharge estimates vary from approximately 30 to 80 mm/a with  
508 the main uncertainty in these values stemming from the challenge of being able to estimate  
509 hydraulic properties at the appropriate spatial scale.

510 Further work will focus on the transferability of this approach to other dryland catchments  
511 which have sufficient groundwater level data available. While we noted in the introduction  
512 that multi-year observations of groundwater dynamics in ephemeral stream catchments are  
513 relatively rare, several data sets appear to show similar features to the data we have presented  
514 here [*Besbes et al.*, 1978; *Carling et al.*, 2012; *Goodrich et al.*, 2004; *Hoffmann*, 2007;  
515 *Houston*, 2002]. Thus we expect that this methodology will be directly applicable to other  
516 catchments. As longer time series become available from the Middle Creek catchment and  
517 others that have recently been established in similar environments, for example as part of the  
518 NCRIS groundwater infrastructure in Australia, the approach will be an important tool to  
519 explore the relationship between groundwater recharge and climate change.

## 520 **Acknowledgements**

521 We are grateful for technical and field support provided by Sam McCulloch, Evan Jensen,  
522 Hamish Studholme, Edwina Davison, Calvin Li and Dong Nguyen and to the landowners -  
523 Philip Laird, Alistair Todd and Steve Bradshaw - for giving access to the field sites. Borehole  
524 and logger installations were only possible by funding from The Australian Federal  
525 Government NCRIS Groundwater Infrastructure Program. Groundwater level and stage data  
526 used in this paper are available at <http://groundwater.anu.edu.au/fieldsite/maules-creek>; daily  
527 rainfall data for Mt Kaputar shown in Figure 7 was downloaded from  
528 <http://www.bom.gov.au/climate/data>; the DEM presented in Figure 6 is used courtesy of  
529 Geoscience Australia - <http://www.ga.gov.au>. MOC was supported by the European  
530 Community's Seventh Framework Programme [FP7/2007-2013] under grant agreement  
531 299091. We are grateful to Greg Pohl, John Nimmo & an anonymous reviewer for their  
532 comments which helped strengthen the manuscript.



533 **References**

- 534 Abdulrazzak, M. J., and H. J. Morel-Seytoux (1983), Recharge from an ephemeral stream following  
535 wetting front arrival to water table, *Water Resources Research*, 19(1), 194-200.
- 536 Acworth, R., G. C. Rau, A. M. McCallum, M. S. Andersen, and M. O. Cuthbert (2014), Understanding  
537 connected surface-water/groundwater systems using Fourier analysis of daily and sub-daily  
538 head fluctuations, *Hydrogeology Journal*, 23(1), 143-159.
- 539 Andersen, M. S., and R. Acworth (2009), Stream-aquifer interactions in the Maules Creek catchment,  
540 Namoi Valley, New South Wales, Australia, *Hydrogeology journal*, 17(8), 2005-2021.
- 541 Besbes, M., J. Delhomme, and G. De Marsily (1978), Estimating recharge from ephemeral streams in  
542 arid regions: a case study at Kairouan, Tunisia, *Water Resources Research*, 14(2), 281-290.
- 543 Bruggeman, G. (1999), *Analytical solutions of geohydrological problems*, Elsevier.
- 544 Carling, G. T., A. L. Mayo, D. Tingey, and J. Bruthans (2012), Mechanisms, timing, and rates of arid  
545 region mountain front recharge, *Journal of Hydrology*, 428, 15-31.
- 546 Currell, M., T. Gleeson, and P. Dahlhaus (2014), A New Assessment Framework for Transience in  
547 Hydrogeological Systems, *Groundwater*.
- 548 Cuthbert, M. (2010), An improved time series approach for estimating groundwater recharge from  
549 groundwater level fluctuations, *Water Resources Research*, 46(9).
- 550 Cuthbert, M. (2014), Straight thinking about groundwater recession, *Water Resources Research*,  
551 50(3), 2407-2424.
- 552 Cuthbert, M., and C. Tindimugaya (2010), The importance of preferential flow in controlling  
553 groundwater recharge in tropical Africa and implications for modelling the impact of climate  
554 change on groundwater resources, *Journal of Water and Climate Change Vol*, 1(4), 234-245.
- 555 Cuthbert, M., and G. Ashley (2014), A Spring Forward for Hominin Evolution in East Africa, *PloS one*,  
556 9(9), e107358.

557 Cuthbert, M., R. Mackay, and J. Nimmo (2013), Linking soil moisture balance and source-responsive  
558 models to estimate diffuse and preferential components of groundwater, *Hydrology & Earth*  
559 *System Sciences*, 17(3).

560 Cuthbert, M., A. Baker, C. N. Jex, P. W. Graham, P. C. Treble, M. S. Andersen, and R. Ian Acworth  
561 (2014), Drip water isotopes in semi-arid karst: Implications for speleothem paleoclimatology,  
562 *Earth and Planetary Science Letters*, 395, 194-204.

563 Dillon, P., and J. Liggett (1983), An ephemeral stream-aquifer interaction model, *Water Resources*  
564 *Research*, 19(3), 621-626.

565 Döll, P., and K. Fiedler (2007), Global-scale modeling of groundwater recharge, *Hydrology & Earth*  
566 *System Sciences Discussions*, 4(6).

567 Domenico, P. A., and F. W. Schwartz (1998), *Physical and chemical hydrogeology*, Wiley New York.

568 Epstein, B., G. Pohl, J. Huntington, and R. Carroll (2010), Development and Uncertainty Analysis of  
569 an Empirical Recharge Prediction Model for Nevada's Desert Basins, *Journal of the Nevada*  
570 *Water Resources Association*, 5(1), 1-22.

571 Goodrich, D. C., D. G. Williams, C. L. Unkrich, J. F. Hogan, R. L. Scott, K. R. Hultine, D. Pool, A. L. Goes,  
572 and S. Miller (2004), Comparison of methods to estimate ephemeral channel recharge, Walnut  
573 Gulch, San Pedro River basin, Arizona, *Groundwater recharge in a desert environment: the*  
574 *southwestern United States*, 77-99.

575 Hantush, M. S. (1967), Growth and decay of groundwater-mounds in response to uniform  
576 percolation, *Water Resources Research*, 3(1), 227-234.

577 Hassan, R. M., R. Scholes, and N. Ash (2005), *Ecosystems and human well-being: current state and*  
578 *trends: findings of the Condition and Trends Working Group*, Island Press.

579 Healy, R. W. (2010), *Estimating groundwater recharge*, Cambridge University Press.

580 Healy, R. W., and P. G. Cook (2002), Using groundwater levels to estimate recharge, *Hydrogeology*  
581 *journal*, 10(1), 91-109.

582 Hoffmann, J. P., Blasch, Kyle W., Pool, Don R., Bailey, Matthew A., and Callegary, James B. (2007),  
583 Estimated infiltration, percolation, and recharge rates at the Rillito Creek focused recharge  
584 investigation site, Pima County, Arizona, in *Ground-water recharge in the arid and semiarid*  
585 *southwestern United States: U.S. Geological Survey Professional Paper 1703-H*, edited, US  
586 Geological Survey.

587 Houston, J. (2002), Groundwater recharge through an alluvial fan in the Atacama Desert, northern  
588 Chile: mechanisms, magnitudes and causes, *Hydrological Processes*, 16(15), 3019-3035.

589 McCallum, A. M., M. S. Andersen, G. C. Rau, J. R. Larsen, and R. I. Acworth (2014), River-aquifer  
590 interactions in a semiarid environment investigated using point and reach measurements,  
591 *Water Resources Research*, 50(4), 2815-2829.

592 Moench, A. F., and C. C. Kisiel (1970), Application of the convolution relation to estimating recharge  
593 from an ephemeral stream, *Water Resources Research*, 6(4), 1087-1094.

594 Nimmo, J. R., J. A. Deason, J. A. Izbicki, and P. Martin (2002), Evaluation of unsaturated zone water  
595 fluxes in heterogeneous alluvium at a Mojave Basin site, *Water Resources Research*, 38(10), 33-  
596 31-33-13.

597 Pool, D. (2005), Variations in climate and ephemeral channel recharge in southeastern Arizona,  
598 United States, *Water resources research*, 41(11).

599 Rau, G. C., M. S. Andersen, A. M. McCallum, and R. I. Acworth (2010), Analytical methods that use  
600 natural heat as a tracer to quantify surface water–groundwater exchange, evaluated using field  
601 temperature records, *Hydrogeology Journal*, 18(5), 1093-1110.

602 Rousseau-Gueutin, P., A. Love, G. Vasseur, N. Robinson, C. Simmons, and G. Marsily (2013), Time to  
603 reach near-steady state in large aquifers, *Water Resources Research*, 49(10), 6893-6908.

604 Scanlon, B. R., K. E. Keese, A. L. Flint, L. E. Flint, C. B. Gaye, W. M. Edmunds, and I. Simmers (2006),  
605 Global synthesis of groundwater recharge in semiarid and arid regions, *Hydrological Processes*,  
606 20(15), 3335-3370.

607 Shanafield, M., and P. G. Cook (2014), Transmission losses, infiltration and groundwater recharge  
608 through ephemeral and intermittent streambeds: A review of applied methods, *Journal of*  
609 *Hydrology*, 511, 518-529.

610 Shentsis, I., and E. Rosenthal (2003), Recharge of aquifers by flood events in an arid region,  
611 *Hydrological Processes*, 17(4), 695-712.

612 Simmers, I. (Ed.) (1997), *Recharge of phreatic aquifers in (semi-) arid areas*, A.A.Balkema, Rotterdam,  
613 Netherlands.

614 Simmers, I. (2003), *Understanding water in a dry environment: hydrological processes in arid and*  
615 *semi-arid zones*, A.A. Balkema, Lisse, The Netherlands.

616 Taylor, R. G., B. Scanlon, P. Döll, M. Rodell, R. Van Beek, Y. Wada, L. Longuevergne, M. Leblanc, J. S.  
617 Famiglietti, and M. Edmunds (2013), Ground water and climate change, *Nature Climate Change*,  
618 3(4), 322-329.

619 Telvari, A., I. Cordery, and D. Pilgrim (1998), Relations between transmission losses and bed alluvium  
620 in an Australian arid zone stream, *Hydrology in a Changing Environment*, 2, 361-366.

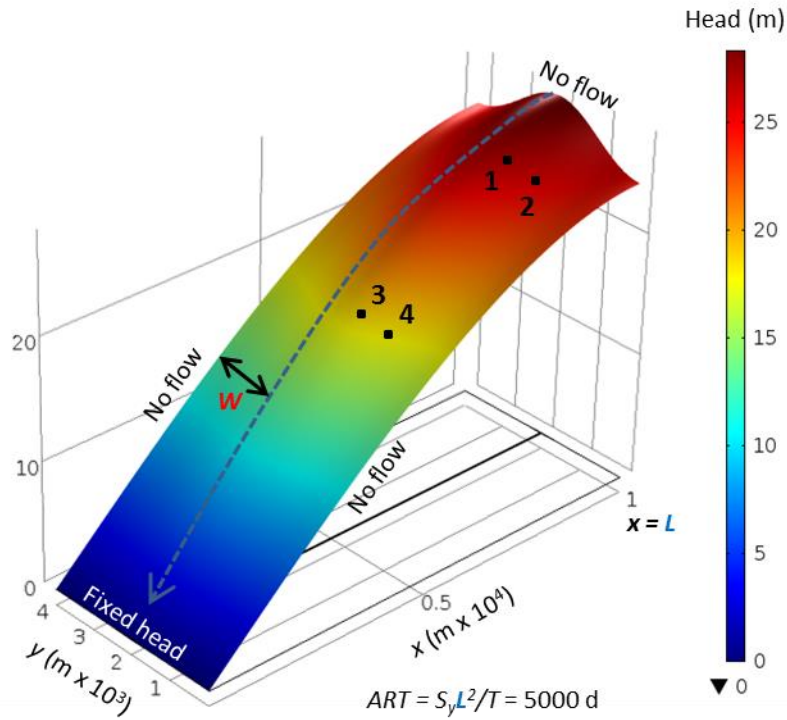
621 Theis, C. V. (1935), The relation between the lowering of the Piezometric surface and the rate and  
622 duration of discharge of a well using ground-water storage, *Eos, Transactions American*  
623 *Geophysical Union*, 16(2), 519-524.

624 van Loon, A., and H. van Lanen (2013), Making the distinction between water scarcity and drought  
625 using an observation-modeling framework, *Water Resources Research*, 49(3), 1483-1502.

626 Venetis, C. (1971), Estimating infiltration and/or the parameters of unconfined aquifers from ground  
627 water level observations, *Journal of hydrology*, 12(2), 161-169.

628 Wheeler, H. S., S. A. Mathias, and X. Li (2010), *Groundwater Modelling in Arid and Semi-Arid Areas*,  
629 Cambridge University Press.

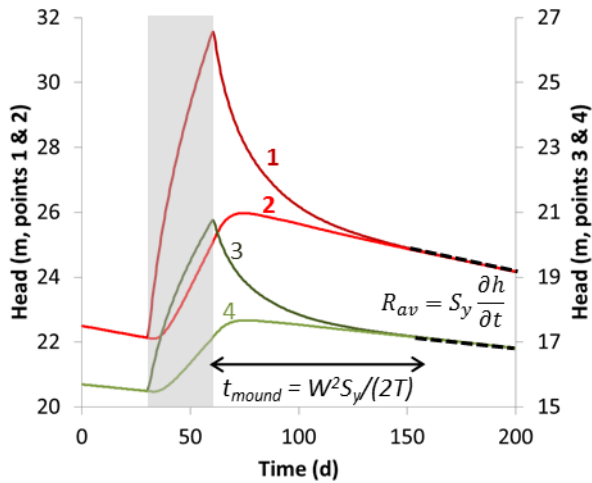
630



631

632 **Figure 1.** Model of an idealised aquifer receiving indirect recharge from an ephemeral  
 633 stream. The parameters used were as follows:  $T = 200 \text{ m}^2/\text{d}$ ,  $S_y = 0.01$ . Dashed blue arrow  
 634 represents the stream recharge boundary. Heads are relative to the fixed head boundary at  
 635  $x = 0$  and represent the water table during a stream flow/recharge event. Numbers 1-4 are  
 636 locations that represent the computed groundwater hydrographs in Fig. 2.

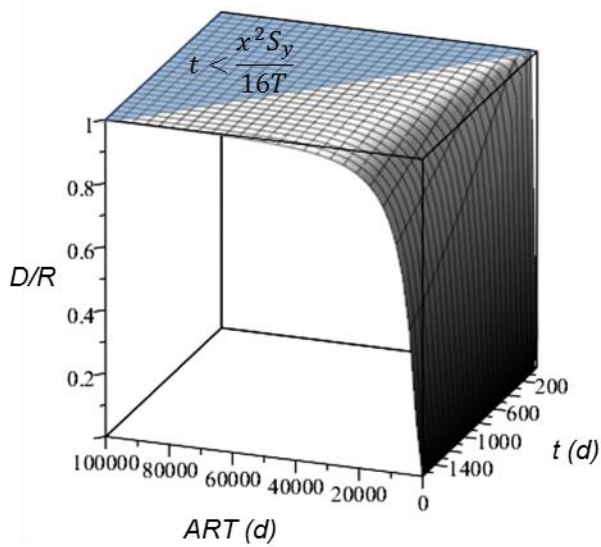
637



638

639 **Figure 2.** Output from the four locations in the model illustrated in Fig.1 showing  
 640 superposition of transverse and longitudinal recessional characteristics. Grey shading  
 641 indicates the period of steady flux input at the stream boundary. Black dashed lines show the  
 642 exact proportionality between the variation of long term (straight line) groundwater head  
 643 recession down the catchment and the long term recharge i.e. the long term recharge rate is  
 644 equal to the specific yield multiplied by the long term head recession rate.

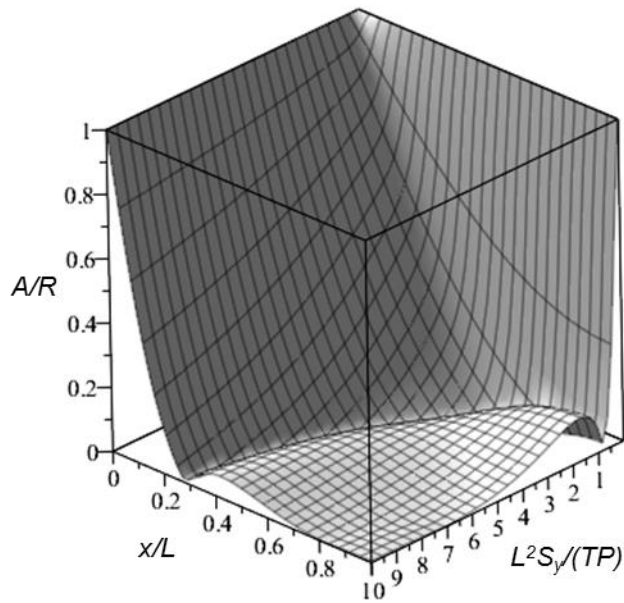
645



646

647 **Figure 3.** Rates of groundwater flux recession ( $D$ ) after recharge ceases normalised to the  
 648 recharge rate ( $R$ ) used to determine the initial conditions, for variations in aquifer response  
 649 time ( $ART = S_y L^2 / T$ ) and time, for a groundwater monitoring point positioned at  $x = 0.5L$ .  
 650 Shaded zone is for  $t < t_{lin}$  as defined by Cuthbert (2014).

651

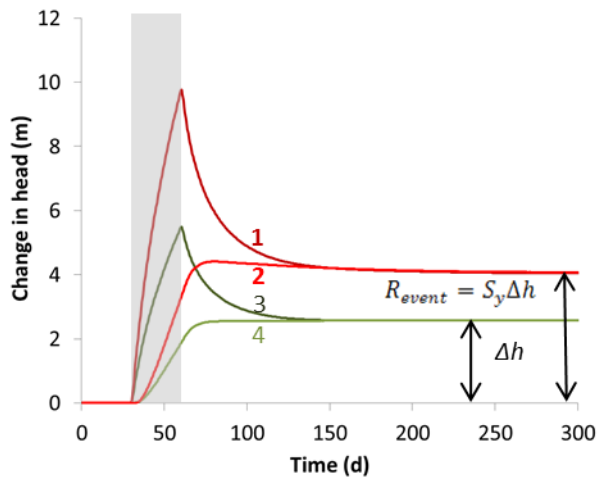


652

653 **Figure 4.** Variation in the amplitude of the flux recession rate ( $A$ ) normalised to the average  
 654 recharge rate ( $R$ ) plotted against the ratio of the ART ( $L^2 S_y / T$ ) to the period of recharge  
 655 variation ( $P$ ) and the position of the groundwater monitoring point with respect to the  
 656 catchment boundaries ( $x/L$ ). Plot created using Equation 8 from Cuthbert (2010). Away from  
 657 the fixed head boundary, ART/ $P$  must be less than 1 for  $A/R$  to deviate significantly (more  
 658 than 10%) from zero. i.e. variations in recharge at periods less than the ART will be damped  
 659 out and not expressed as variations in the flux recession rate.

660

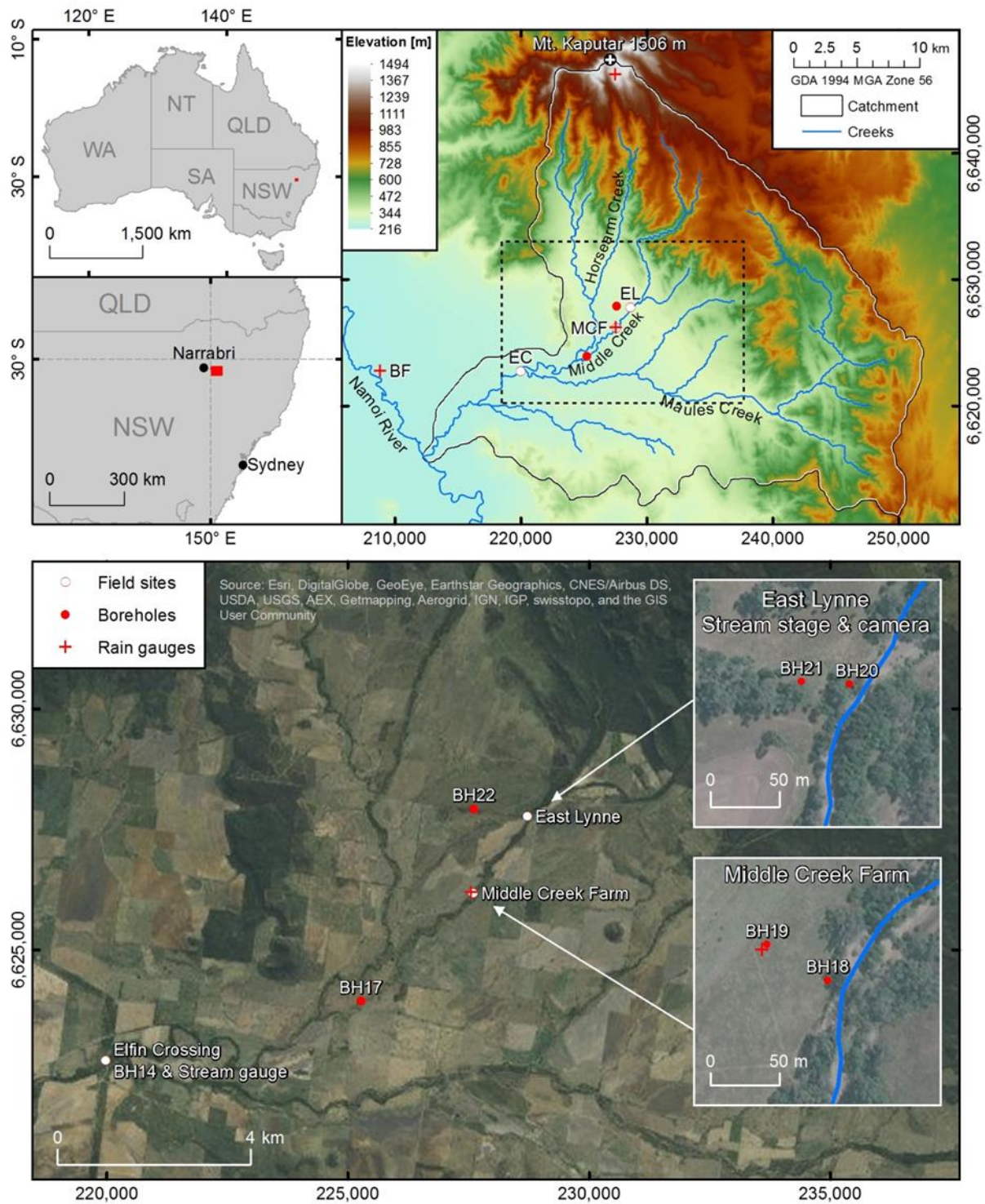




661

662 **Figure 5.** Groundwater hydrographs for the cases shown in Figure 2 with the long term  
 663 recession removed to reveal the effects solely due to recharge from the stream. Grey shading  
 664 indicates the period of steady flux input at the stream boundary.

665



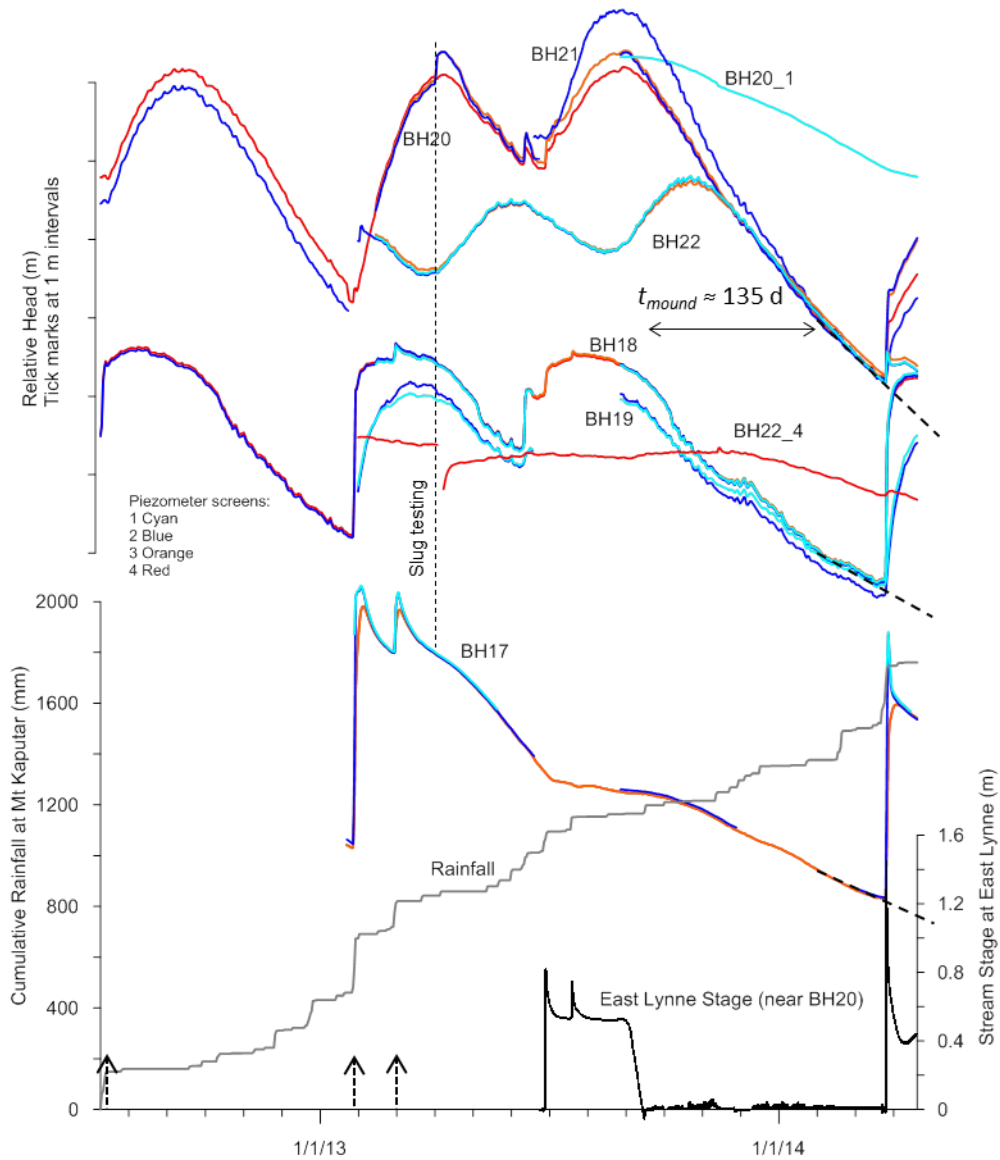
666

667 **Figure 6.** Middle Creek and monitoring installations in the context of the Maules Creek

668 catchment. DEM used courtesy of Geoscience Australia. BF = Bellevue Farm; EC = Elfin

669 Crossing; MCF = Middle Creek Farm; EL = East Lynne.

670



671

672 **Figure 7.** Groundwater hydrographs (daily average), stream stage and cumulative rainfall.

673 Heads are given on the same vertical scale, but with the absolute values shifted to enable the

674 hydrographs to be compared. Dashed black arrows indicate stream flow events at East Lynne

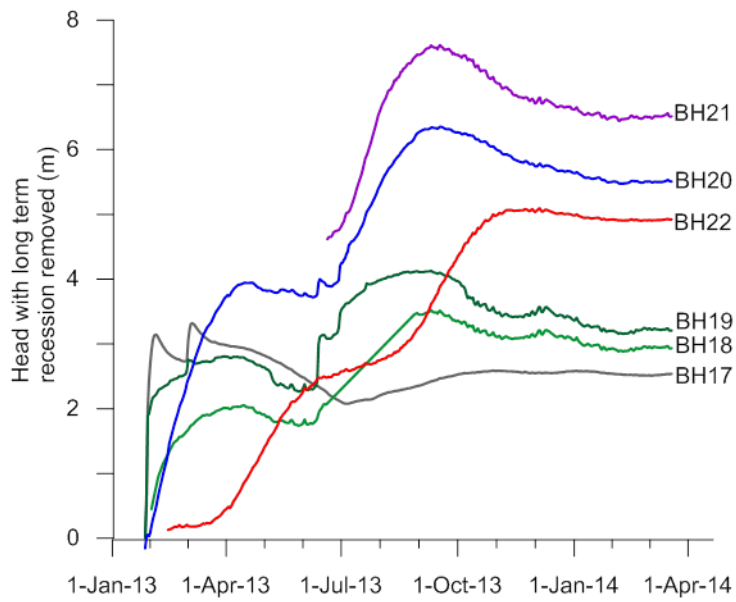
675 (BH20-21) captured by an automatic camera, prior to the installation of stream stage

676 monitoring. Bold dashed black lines indicate periods of straight line groundwater recession.

677 The different piezometer screens for each borehole are coloured according to the key shown

678 with 1-4 being shallow to deep respectively. The time of slug testing is also marked as it led

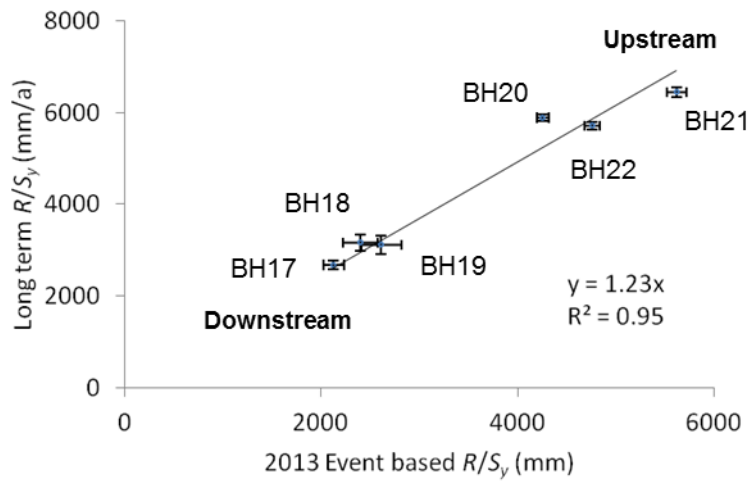
679 to a temporary disturbance of the natural heads.



680

681 **Figure 8.** Groundwater hydrographs with background recessions 'removed'. The final head  
 682 value represents the increase due to recharge from ephemeral stream flow since Jan 13.  
 683 Where continuous data were not available from data loggers (i.e. BH22, BH19 & BH21), the  
 684 residual heads were calculated using dip-tape measurements taken just prior to the stream  
 685 flow event in late Jan 2013.

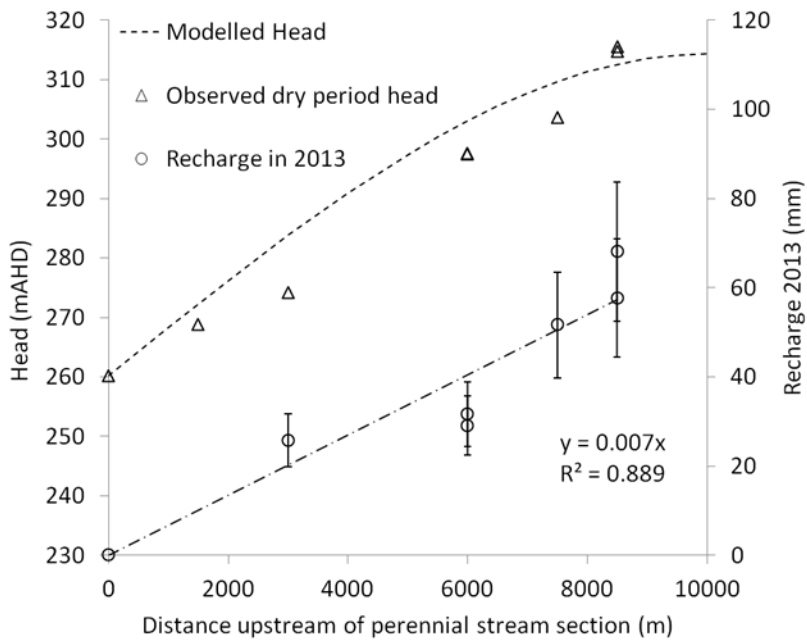
686



687

688 **Figure 9.** Comparison of long term and event based indirect recharge estimates.

689



690

691 **Figure 10.** Variation of estimated recharge with distance upstream and comparison of  
 692 observed dry period heads (i.e. during a straight line recession period) with heads predicted  
 693 using Equation 4.

	Recession rate	Residual head increase for 2013	Error in estimated value of $R/S_y$	Long term recharge	Recharge in 2013	Error in recharge
BH17	2678	2123	104	32	25	5.9
BH18	3118	2609	154	37	31	7.3
BH19	3166	2398	175	38	29	6.7
BH20	5711	4757	75	69	57	13.2
BH21	6444	5618	96	77	67	15.6
BH22	5892	4258	64	71	51	11.8

694

695 *Table 1 Summary of recession rates and recharge estimates - all values in mm/a*

696

697